INTERNATIONAL JOURNAL FOR NUMERICAL AND ANALYTICAL METHODS IN GEOMECHANICS
Int. J. Numer. Anal. Meth. Geomech., **22**, 1021–1033 (1998)

SHORT COMMUNICATION

THE EFFECT OF INTERFACE PROPERTIES ON RETAINING WALL BEHAVIOUR

R. A. DAY[1,*] AND D. M. POTTS[2]

[1]*Department of Civil Engineering, The University of Queensland, Brisbane 4072, Australia*
[2]*Department of Civil Engineering, Imperial College of Science Technology and Medicine, Imperial College Road, London SW7 2BU, U.K.*

SUMMARY

A series of finite element analyses have been undertaken to investigate the effects of interface properties on the behaviour of a vertical retaining wall and the deformation of the ground around it. The boundary between a rigid embedded wall and the soil is modelled with zero thickness interface elements. Uniform translation of the wall has been studied. The analyses show the predicted limiting active and passive pressure on the wall are dependent on the maximum wall friction angle and are in reasonable agreement with accepted approximate analytical solutions. The limiting pressure is independent of the stiffness and dilation properties of the interface elements. The dilation properties of the interface have a significant effect on the ground surface deformation around the wall. © 1998 John Wiley & Sons, Ltd.

Key words: retaining wall; interface; finite element

1. INTRODUCTION

Potts and Fourie[1] have carried out a numerical study of the effects of wall deformation on earth pressure. They however did not use interface elements and consequently performed analyses assuming fully rough and fully smooth walls only. This paper extends their work for the case of uniform horizontal wall translation. A finite element study was undertaken using interface elements to investigate the effects of interface properties on the behaviour of a retaining wall. The influence of maximum wall friction angle, interface stiffness, and interface dilation, on the active and passive earth pressure coefficients, the failure mechanism and the deformed soil surface profile is studied. The numerically calculated earth pressure coefficients are compared with various approximate analytically derived values used in retaining wall analysis and design.

2. DETAILS OF ANALYSES

A rigid wall embedded 5 m into the soil was translated uniformly in the horizontal direction. Interface elements placed on both sides of the wall allowed the magnitude of the maximum angle

Correspondence to: R. A. Day, Department of Civil Engineering, The University of Queensland, Brisbane 4072, Australia, Tel.: + 61 (0)7 3365 3896, Fax: + 61 (0)7 3365 4599, Email: r.day@mailbox.uq.edu.au

CCC 0363–9061/98/121021–13$17.50

Received 18 July 1997
Revised 3 February 1998

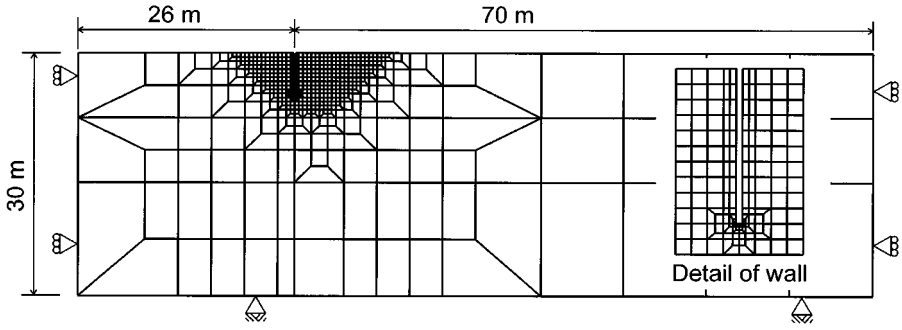

Figure 1. Finite element mesh

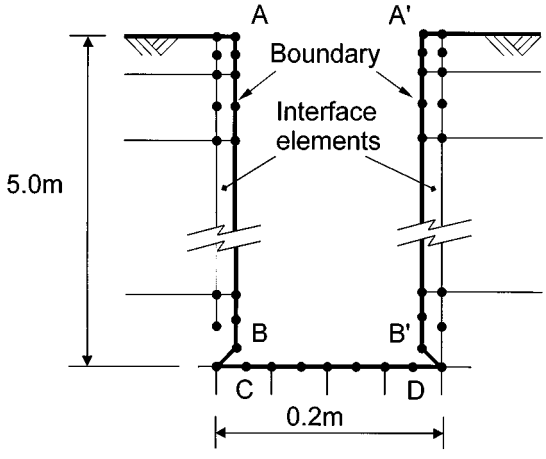

Figure 2. Boundary details at wall

of wall friction, δ, and amount of joint dilation to be varied. The minimum active force, the maximum passive force, the failure surfaces and the deformed profile of the soil surface are compared.

The finite element mesh used in the analysis and the applied boundary constraints are shown in Figure 1. The soil was modelled with 8 node isoparametric 2-D elements[2] and the interface was modelled with 6 node relative displacement 1-D interface elements.[3–5] The rigid wall was modelled as part of the boundary. A detail of the mesh around the bottom of the wall is shown in Figure 2. The nodes on the boundaries A–B, A′–B′ and C–D were moved horizontally to the right under displacement control. A total of 120 mm displacement was applied. Vertical displacement of these nodes was not permitted.

The Mohr–Coulomb failure criterion was adopted as the yield function for the soil. The material properties of the soil are the same as those used by Potts and Fourie.[1] These are: $E = 60\,000\ \mathrm{kN/m^2}$, $\mu = 0{\cdot}2$, $c' = 0$, $\phi' = 25^\circ$. Fully associated plastic flow was assumed for the soil. The bulk unit weight $\gamma = 20\ \mathrm{kN/m^3}$. The initial horizontal stress was assumed to be equal to the vertical stress ($K_0 = 1{\cdot}0$) . Fully drained plane strain analyses were performed.

Table I. Interface element properties

Analysis no.	Stiffness, K_s, K_n (kN/m^3)	Friction, δ (deg)	Dilation, v (deg)
			Associated
1	E	25·0	25·0
2	$100E$	25·0	25·0
9	E	22·5	22·5
10	E	20·0	20·0
4	E	17·5	17·5
5	E	12·5	12·5
6	E	5·0	5·0
8	E	0·0	0·0
			Non-associated
3	E	25·0	0·0
7	E	5·0	0·0

E is the value of the Young's modulus of the soil in kN/m^2.

The Mohr–Coulomb failure criterion with zero cohesion was also adopted as the yield surface for the interface elements. Fully associated and non-dilatant interface element behaviour has been considered. Table I gives the interface element properties used in each analysis. An analysis in which there were no interface elements was also performed.

2.1. *Quality of solution*

This problem, particularly when high values of wall friction and associated soil behaviour are specified, is difficult to solve using numerical methods. Because of the kinematic constraints on the soil adjacent to the wall, there is little freedom for the solution to redistribute the residual, or out of balance stress.

Displacement control was used for the analyses presented here. An accelerated modified Newton–Raphson scheme with a sub-stepping stress point algorithm was employed to solve the non-linear finite element equations.[6] The magnitude of the out-of-balance stress at the end of the analysis was checked to ensure adequate accuracy of the solution.

3. RESULTS OF ANALYSES

3.1. *Earth pressure coefficients*

Figure 3 shows the development of active and passive earth pressure coefficients in analyses 1 and 3–10 as the wall displacement is increased. The equivalent earth pressure coefficient, K, is calculated from $K = 2P_h/(\gamma H^2)$. H is the height of the wall and P_h is the force per unit length of wall calculated from the sum of the horizontal nodal reactions along the boundary representing the wall. Calculation of the reaction considered the stress only in the elements adjacent to the wall. The limiting values of K, i.e. K_{ah} and K_{ph}, are listed in Table II.

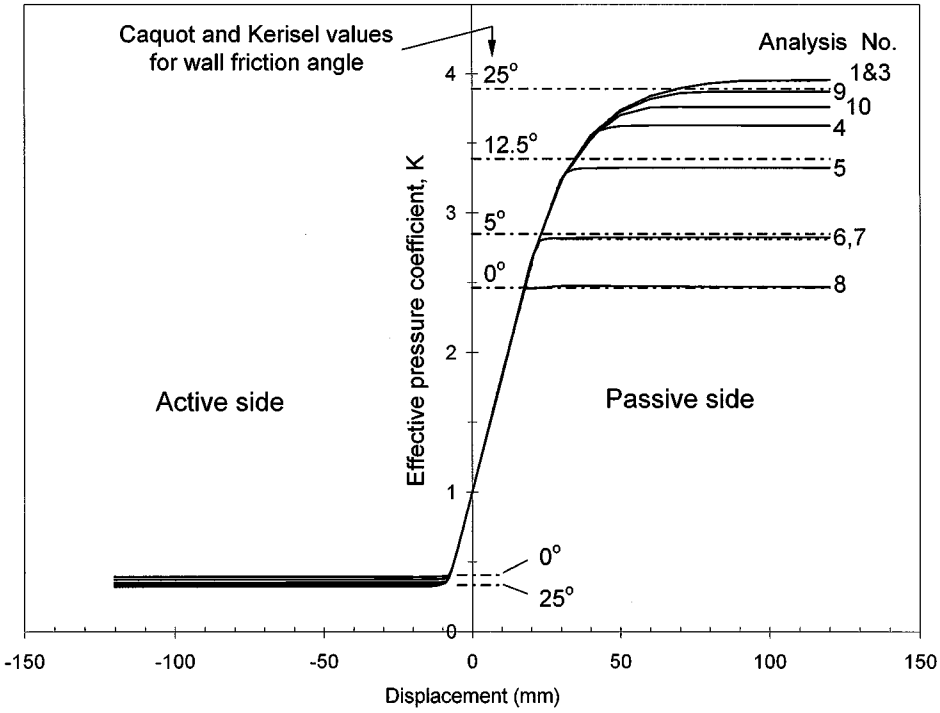

Figure 3. Effective pressure coefficient—analyses 1 and 3–10

Table II. Calculated K_a and K_p values

Analysis no.	Active pressure			Passive pressure		
	Horizontal K_{ah}	Resultant k_a	Wall friction	Horzional K_{ph}	Resultant K_p	Wall friction
No interface element	0·303	0·331	23·7	3·98	4·40	25·4
1	0·323	0·355	24·7	3·96	4·36	24·9
2	0·324	0·356	24·4	3·98	4·39	25·0
3	0·323	0·355	24·8	3·95	4·36	24·9
9	0·328	0·354	22·3	3·87	4·19	22·5
10	0·333	0·354	19·9	3·76	4·00	20·0
4	0·339	0·355	17·5	3·63	3·80	17·5
5	0·351	0·360	12·5	3·32	3·41	12·5
6	0·373	0·374	5·0	2·82	2·83	5·0
7	0·373	0·374	5·0	2·81	2·82	5·0
8	0·392	0·392	0·0	2·47	2·47	0·0

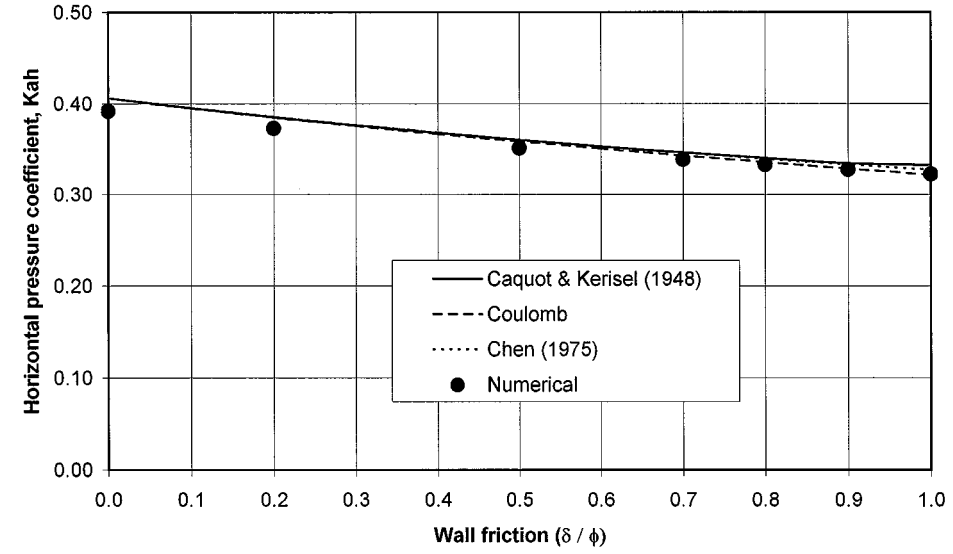

(a) **Horizontal component of Active pressure**

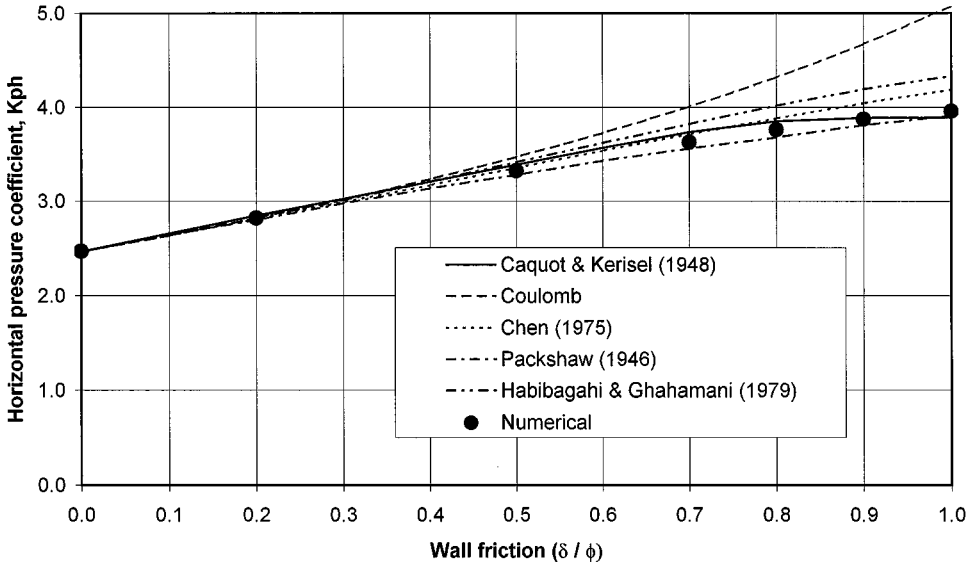

(b) **Horizontal component of passive pressure**

Figure 4. Comparison of pressure coefficients: (a) active pressure; (b) passive pressure

The angle of wall friction given in Table II is calculated from $\tan^{-1}(P_v/P_h)$ where P_v and P_h are the sum of the vertical and horizontal reactions along the boundary representing the wall. It is therefore the angle from horizontal of the direction of the resultant reaction. On the passive side of the wall, friction is fully mobilized over the full length of the wall. On the active side the average mobilized wall friction is slightly less than the maximum. This is likely to be caused by fluctuations in the soil stress (see discussion below on earth pressure) due to large stress and strain gradients in the elements around the base of the wall.

The magnitude of the average wall friction on the passive side in the analysis without interface elements is greater than 25°. This does not satisfy the soil constitutive model. The friction angle has been calculated from the horizontal and vertical reactions on the boundary representing the face of the wall. The reactions are indirectly determined by extrapolating the integration point stresses to the boundary. The integration point stresses satisfy the constitutive law. The extrapolated boundary stresses and reactions do not necessarily satisfy the constitutive law, particularly if high stress gradients exist. The integration points for the zero thickness interface elements are on the interface and therefore no extrapolation towards the wall is necessary. Hence, the interface stress and the average angle of wall friction satisfy the constitutive law.

It is clear that the ultimate earth pressure coefficients are dependent on the maximum wall friction angle (as expected) but are independent of the dilation and the elastic stiffness of the interface.

The calculated values of K_{ph} and K_{ah} are compared with various approximate analytical methods in Figure 4. The analytical values of K_{ah} are all very similar and have little variation due to wall friction. The finite element values are slightly lower than all of the analytical methods for all values of wall friction angle. The differences are however quite small. The various analytical values of K_{ph} are similar at low friction angles (for $\delta = 0$ they are all equal) but have a substantial variation for a fully rough wall. The values calculated by the finite element analyses with the interface element are in reasonable agreement with those of Caquot and Kerisel,[7] Chen[8] and Packshaw[9] at all values of wall friction. The values given by Packshaw are slightly less, and the values given by Chen are greater than the finite element values at all wall friction angles. As is widely agreed, the values given by Coulomb[10] overestimate K_{ph} considerably for higher wall friction angles.

3.2. *Earth pressure*

Figure 5 shows the distribution of normal stress in the interface element at the end of the analysis. Since friction is fully mobilized at all points on the back of the wall, the distribution of shear stress is similar. Some oscillation of the integration point stress occurs in the bottom two elements. This is likely to be due to very large strains and high stress gradients in the soil elements around the base of the wall. At the base of the wall the horizontal stress in the soil changes from about 400 kPa on the passive side to about 40 kPa on the active side over the width of the wall (0·2 m).

The ultimate stress distribution on both sides of the wall is nearly linear in each analysis. A linear distribution is generally assumed in the analytical earth pressure theories. Towards the base of the wall the passive pressure tends to be greater than, and the active pressure less than, an equivalent linear distribution.

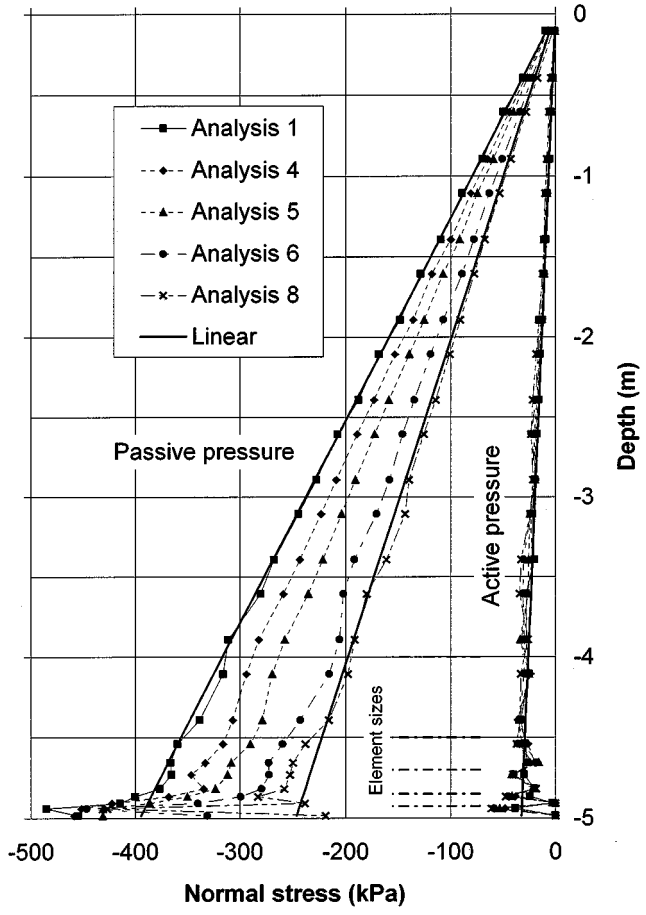

Figure 5. Normal stress on wall

3.3. *Failure mechanism*

The failure mechanism is indicated by the vectors of incremental displacement in the last increment of the analysis. Figure 6 shows the failure mechanism for analyses 3 and 7 in which the interface has no dilation. In the corresponding analyses with the same interface friction but with a fully associated interface (analyses 1 and 6, respectively) the active and passive failure surfaces are in similar locations as the case of no joint dilation. All soil movement occurs within a similar shaped failure 'wedge'. The value of interface dilation does not affect the location of the failure surface through the soil.

For analysis 7 ($\delta = 5^\circ$) the failure surfaces are close to planes subtending angles to the horizontal of $45 + \phi'/2$ and $45 - \phi'/2$ on the active and passive sides, respectively. For analysis 3 ($\delta = \phi'$) the failure surface on the passive side is curved. It begins at the bottom of the wall in a slightly downwards direction and emerges at the soil surface at an angle of about $45 - \phi'/2$ to the horizontal. The results of the other analyses indicate failure surfaces between these two

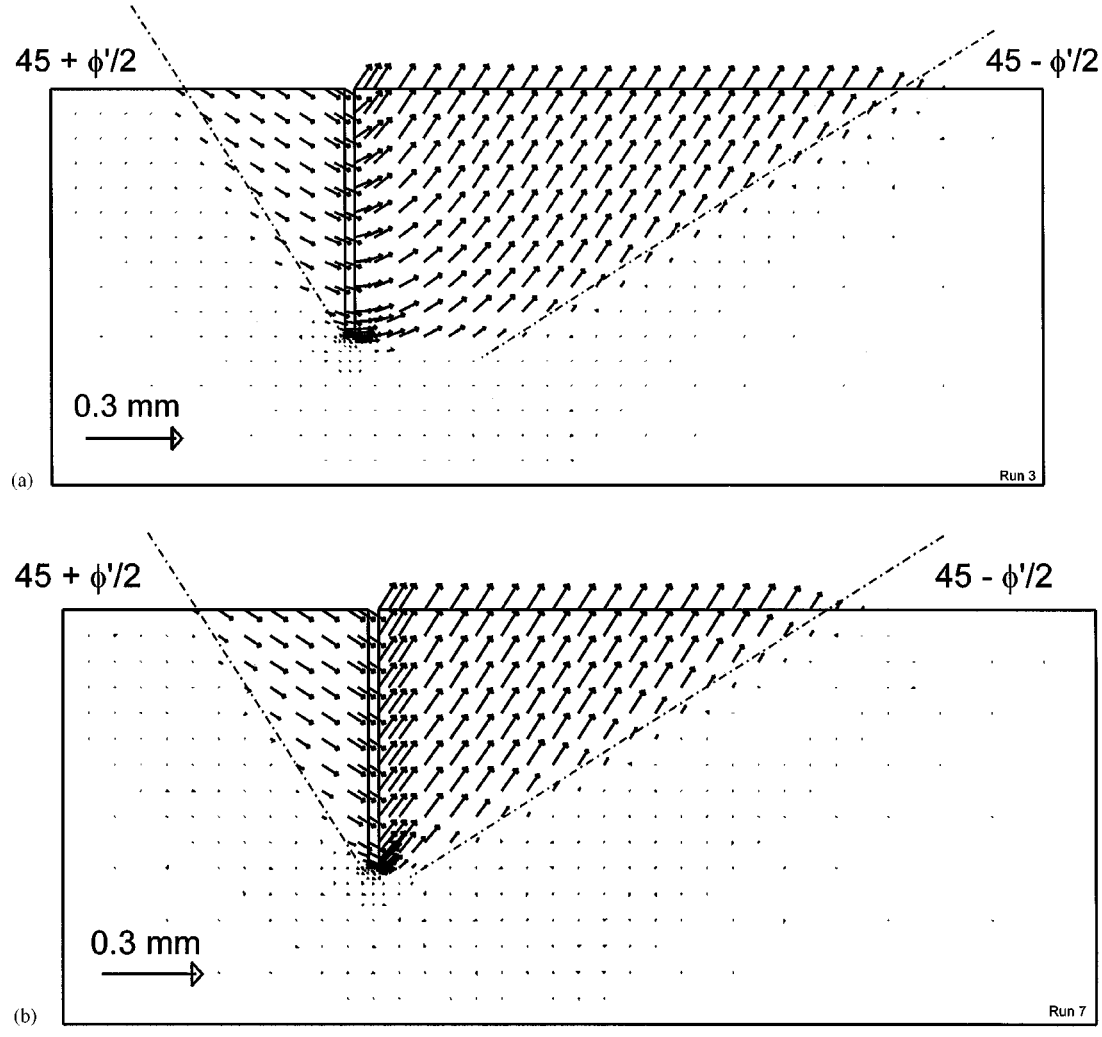

Figure 6. Vectors of failure displacement, no interface dilation: (a) wall friction = 25° (Analysis No. 3); (b) wall friction = 5° (Analysis No. 7)

extremes. These results agree with analytical limit equilibrium[7] and limit analysis[8] methods which also indicate failure on plane surfaces for smooth walls ($\delta = 0$) and curved surfaces (eg. log spiral) for rough walls ($\delta = \phi'$).

3.4. Displaced soil surface profile

Figure 7 compares the analyses assuming full wall friction (Analyses 1 and 2) with the analysis in which there were no interface elements. The differences in the vertical displacement of the soil

adjacent to the wall are due to slip in the interface element. In the analyses without interface elements the vertical displacement of the soil beside the wall is zero. Because, the interface elements allow slip to occur beside the wall, there is a vertical displacement of the soil adjacent to the wall in these analyses. The differences in the horizontal displacement of the soil adjacent to the wall are due to dilation of the interface. When interface elements are not present, the horizontal displacement of the soil adjacent to the wall is equal to the prescribed displacement of 120 mm. Analyses 1 ($K_n = E$) and 2 ($K_n = 100E$) are essentially the same as the analysis without interface elements.

Figure 8 shows the effect of wall friction and interface dilation on the deformed soil surface profile. The rapid change in the displaced shape that occurs at 2–4 m from the wall on the active side and at 8–12 m from the wall on the passive side is where the failure surface intersects the soil surface.

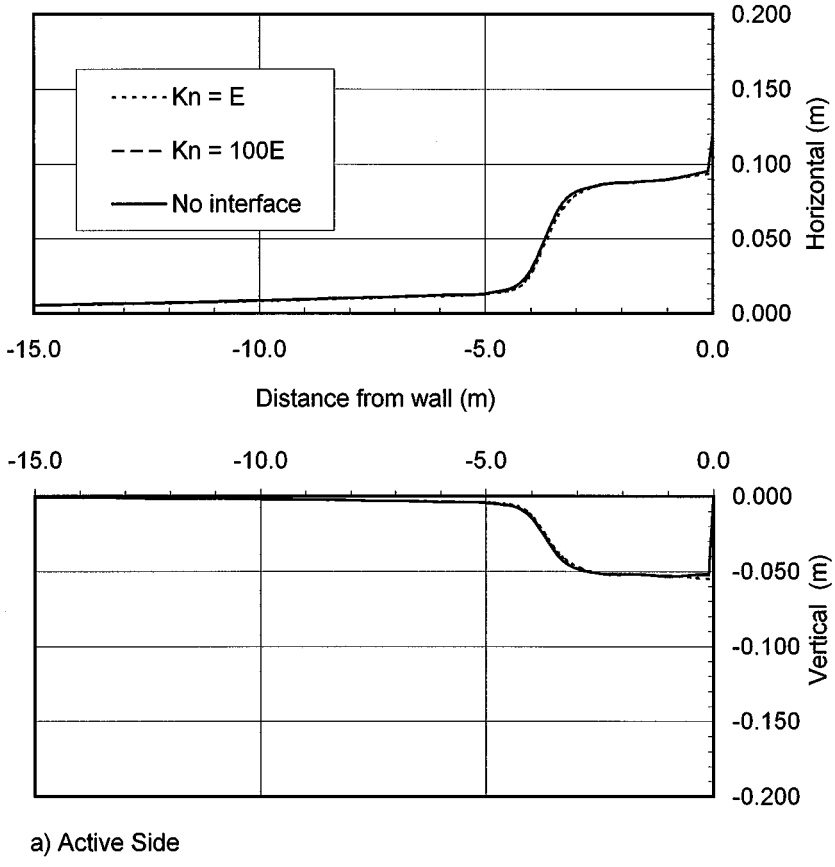

Figure 7. Surface movement–effect of joint stiffness: (a) active side; (b) passive side

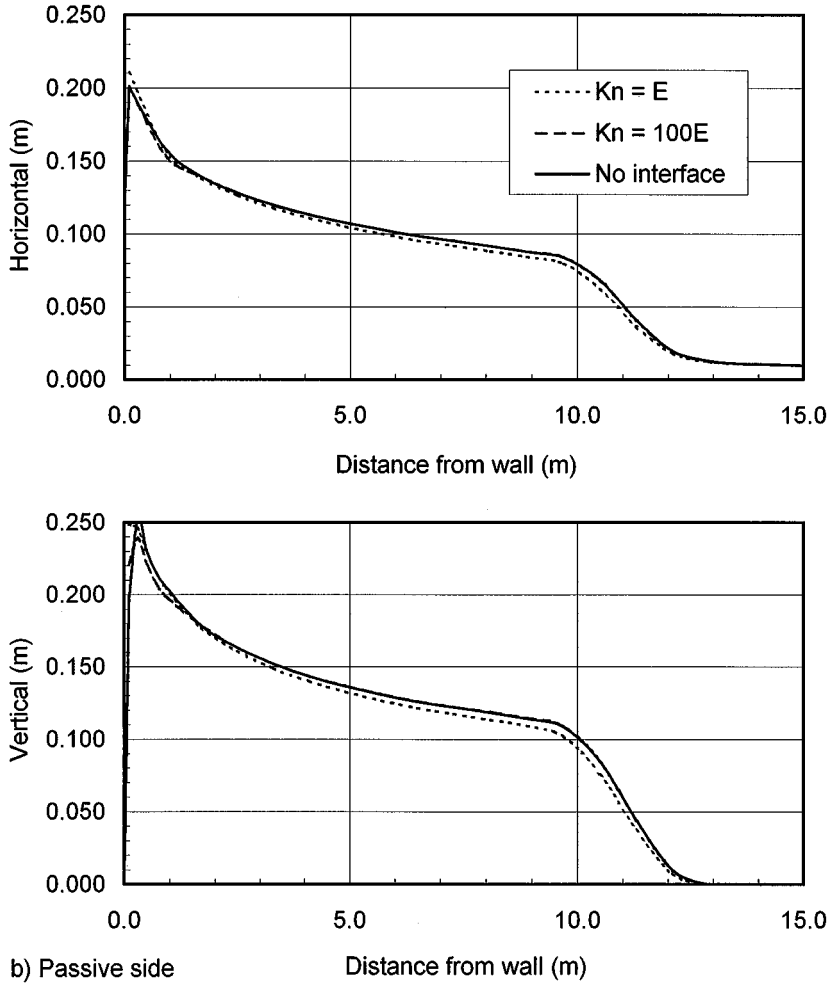

Figure 7. Continued

Dilation of the interface has a marked effect on the soil surface profile. For the case of the rough wall, it accounts for approximately 40% of the horizontal and vertical displacement of the soil immediately adjacent to the wall on the passive side (compare analyses 1 and 3). The gradient of the soil surface profile (both horizontal and vertical) between the wall and the failure surface is dependent on the dilation of the interface element. The distance from the wall to the position of the failure surface is essentially independent of the interface dilation but dependent on the maximum wall friction angle.

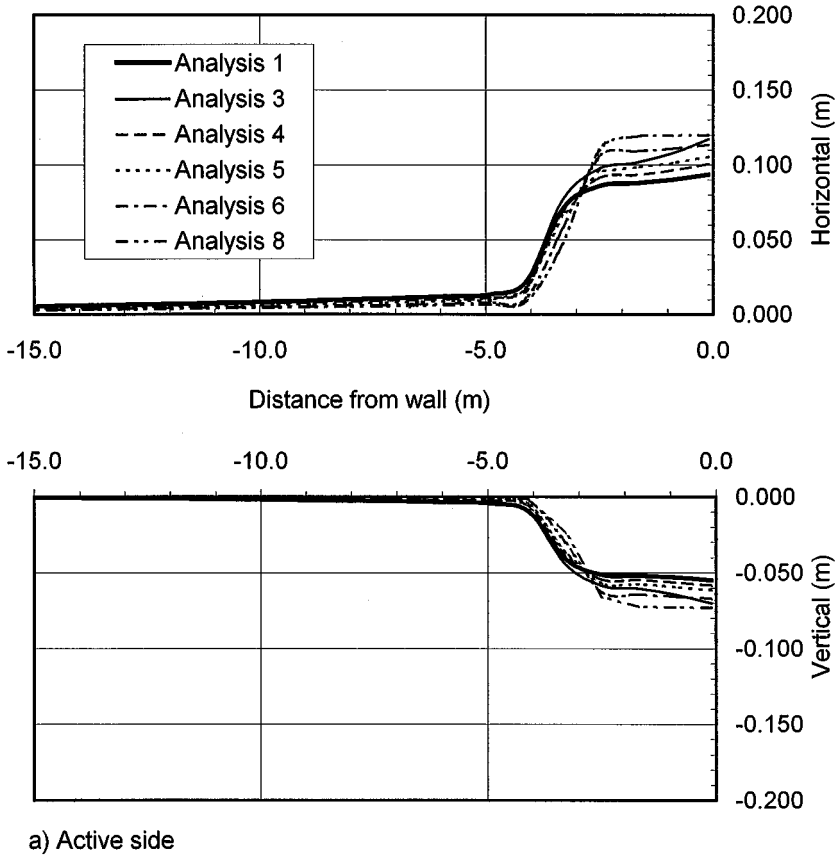

Figure 8. Surface movement–effect of joint friction and dilation: (a) active side; (b) passive side

4. CONCLUSION

The use of interface elements with a simple elasto-plastic Mohr–Coulomb failure criterion has predicted ultimate values of earth pressure for various angles of wall friction in reasonable agreement with analytical solutions. These analyses have provided numerical confirmation of the analytical solutions such as Caquot and Kerisel that are widely accepted and commonly used in retaining wall design. These values however apply only to the situation of uniform wall translation. Different modes of wall movement, for example rotation, will affect the ultimate value and distribution of the earth pressure on the wall.

In the analysis of the active and passive failure modes of a retaining wall, the ultimate earth pressure is independent of the elastic stiffness and the angle of dilation of the interface elements. But the angle of dilation has a significant effect on the deformed soil surface profile. The results obtained for a fully rough wall modelled with interface elements assuming associated plastic flow are essentially the same as those obtained if no interface element is used on the soil–wall boundary.

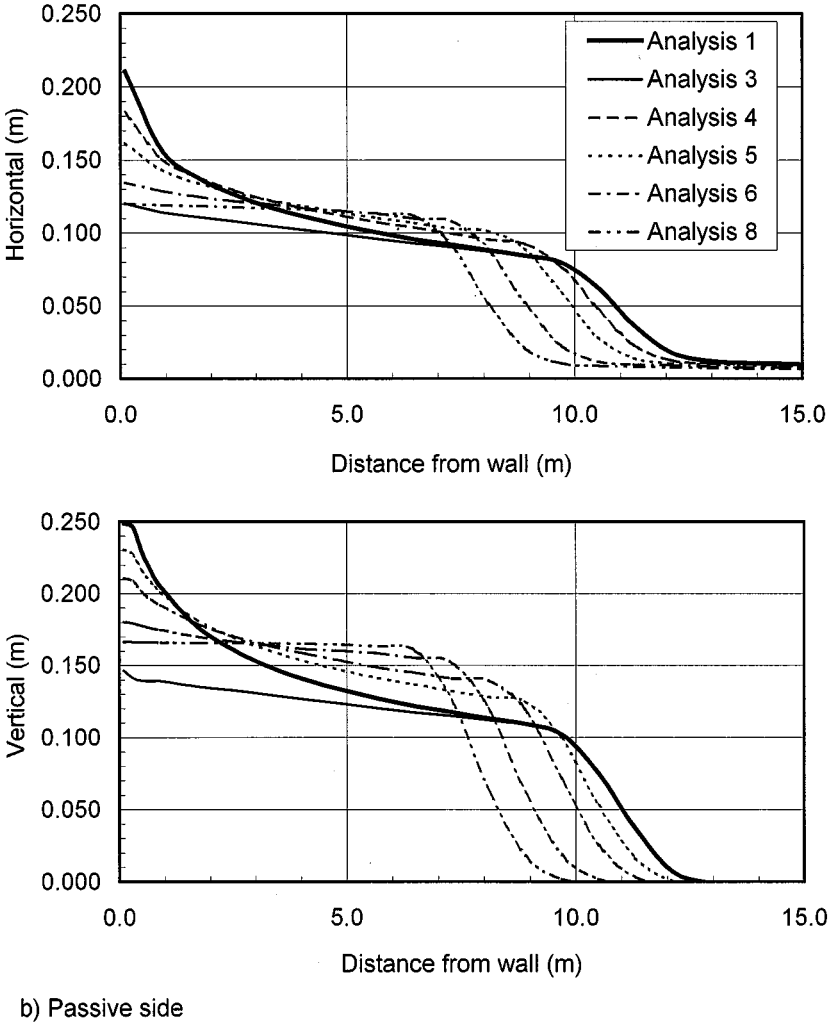

Figure 8. Continued

The interface element provides a useful means to model reduced interface friction and non-associated interface behaviour in finite element analysis of retaining walls. The simple elasto-plastic Mohr–Coulomb constitutive model appears to be satisfactory for the modelling of interface behaviour in this type of analysis.

REFERENCES

1. D. M. Potts and A. B. Fourie, 'A numerical study of the effects of wall deformation on earth pressures', *Int. J. Numer. Anal. Meth. Geomech.*, **10,** 383–405 (1986).
2. O. C. Zienkiewicz, *The Finite Element Method*, 3rd edn, McGraw-Hill, London, 1977.
3. I. Carol and E. E. Alonso, 'A new joint element for the analysis of fractures rock', *5th Int. Congress on Rock Mechanics*, **F**, Melbourne, 1983, pp. 147–151.

4. A. Gens, I. Carol and E. E. Alonso, 'An interface element formulation for the analysis of soil-reinforcement interaction', *Comput. Geotech.*, **7,** 133–151 (1989).
5. A. Gens, I. Carol and E. E. Alonso, 'A constitutive model for rock joints formation and numerical implementation', *Comput. Geotech.*, **9,** 3–20 (1990).
6. D. M. Potts and D. Genendra, 'An evaluation of sub-stepping and implicit stress point algorithms'. *Comput. Meth. Appl. Mech. Eng.*, **119,** 341–354 (1994).
7. A. Caquot and J. Kerisel, *Tables for the Calculation of Passive Pressure, Active Pressure and Bearing Capacity of Foundations*, Gauthier-Villars, Paris, 1948.
8. W. F. Chen, 'Limit analysis and soil plasticity', *In Developments in Geotechnical Engineering*, Vol. 7, Elsevier, Amsterdam, (1975).
9. E. Packshaw, 'Earth pressure and earth resistance', *J. ICE*, **25,** 233–256 (1946).
10. C. A. Coulomb, 'Essai sur une application des regles de maximis et minimus a quelques Problemes de statique, relatifs a l'architecture'. *Memoires de Mathematique et de Physique Presentes a l'Academie Royale des Sciences*, Vol. 7, Paris, 1776.

